Journal of Molecular Structure 963 (2010) 137–144

Contents lists available at ScienceDirect

Journal of Molecular Structure

journal homepage: www.elsevier.com/locate/molstruc

Vibrational spectra and computational study of 3-amino-2-phenyl quinazolin-4(3*H*)-one

C. Yohannan Panicker [a],*, Hema Tresa Varghese [b], K.R. Ambujakshan [c], Samuel Mathew [d], Subarna Ganguli [e], Ashis Kumar Nanda [f], Christian Van Alsenoy [g], Y. Sheena Mary [h]

[a] Department of Physics, TKM College of Arts and Science, Kollam, Kerala 691005, India
[b] Department of Physics, Fatima Mata National College, Kollam, Kerala 691001, India
[c] Department of Physics, MES Ponnani College, Ponnani South, Malappuram, Kerala, India
[d] Department of Physics, Mar Thoma College, Thiruvalla , Kerala 689103, India
[e] Calcutta Institute of Pharmaceutical Technology and Allied Health Sciences, Banitabla, Uluberia, Howrah-711316, West Bengal, India
[f] Department of Chemistry, North Bengal University, Raja Rammohunpur, Siliguri 734013, West Bengal, India
[g] University of Antwerp, Chemistry Department, Universiteitsplein 1, B2610 Antwerp, Belgium
[h] Thushara, Neethinagar-64, Pattathanam, Kollam, Kerala, India

ARTICLE INFO

Article history:
Received 8 September 2009
Received in revised form 15 October 2009
Accepted 15 October 2009
Available online 20 October 2009

Keywords:
Quinazoline
IR
Raman
HF
DFT calculations
PED

ABSTRACT

FT-Raman and FT-IR spectra of 3-amino-2-phenyl quinazolin-4(3*H*)-one were recorded and analyzed. The vibrational wavenumbers of the title compound have been computed using the Hartree–Fock/6-31G* and B3LYP/6-31G* basis sets and compared with the experimental data. The prepared compound was identified by NMR and mass spectra. The red shift of the NH stretching wavenumber indicates the weakening of the NH bond. The simultaneous IR and Raman activation of the C=O stretching mode gives the charge transfer interaction through a π-conjugated path. The first hyperpolarizability, Infrared intensities and Raman activities are reported. The calculated first hyperpolarizability is comparable with the reported values of similar derivatives and is an attractive object for future studies of non-linear optics. The assignments of the normal modes are done by potential energy distribution (PED) calculations. Optimized geometrical parameters of the title compound are in agreement with reported similar structures.

© 2009 Elsevier B.V. All rights reserved.

1. Introduction

Quinazolines are frequently used in medicine because of their wide spectrum of biological activities [1]. Compounds containing a fused quinazoline or isoquinoline ring belong to a broad class of compounds that has received a considerable attention over the past years due to their wide range of biological activities [2,3]. Some of the aminoquinazoline derivatives were found to be inhibitors of the tyrosine kinase [4,5] or dihydrofolate reductase enzymes [6,7] and so they work as potent anticancer agents. They are also used to design medicines against hypertension and malaria and to fight infections involving acquired immune deficiency syndrome (AIDS) [8]. Among a wide variety of nitrogen heterocycles that have been explored for developing pharmaceutically important molecules, the quinazolines have played an important role in the medicinal chemistry and subsequently emerged as a pharamacophore [9]. In normal practice, three groups of agents (chemotherapeutic, analgesic and anti-inflammatory) are prescribed simultaneously. Compounds possessing all three activities are not common. Quinazolines and quinazoline derivatives exhibit potent antimicrobial [10] and central nervous systems activities such as anti-inflammatory [11] and anticonvulsant [12]. Anti-tumor activities are also reported for 2,3-dihydro-2-aryl-4-quinazolines [13,14]. Several quinazoline derivatives have been reported for their antibacterial, antifungal, anti-Human Immunodeficiency Virus (HIV) [15,16], anthelmintic [17], central nervous system depressant [18], antitubercular [19], hypotensive [20], anticonvulsant [21], anti-fibrillatory [22], diuretic [23] and antiviral activities [24–26]. Some reports have suggested that 2-styrylquinazolin-4-ones [27,28] could be effective inhibitors of tubulin polymerization. The 2,3-disubstituted quinazolones have been predicted to possess antiviral and antihypertensive activities [29]. Synthesis of vascinone, a naturally occurring bioactive alkaloid having a quinazolone system, has been reported recently [30]. Quinazolines are widely used for the extraction and analytical determination of metal ions. Nitraquazone, a quinazoline derivative, has been found to possess potent phosphodiesterase inhibitory activity [31] which is potentially useful in the treatment asthma [32]. Alagarsamy et al. [33] have reported the synthesis and analgesic, anti-inflammatory and antibacterial activities of

---

* Corresponding author.
E-mail address: cyphyp@rediffmail.com (C.Y. Panicker).

0022-2860/$ - see front matter © 2009 Elsevier B.V. All rights reserved.
doi:10.1016/j.molstruc.2009.10.026

some novel 2-phenyl-3-substituted quinazolin-4(3*H*)-ones. Costa et al. [34] reported the synthesis of 4*H*-3,1-benzoxazines, quinazolin-2-ones and quinoline-4-ones by palladium-catalyzed oxidative carbonylation of 2-ethynylaniline derivatives. These nitrogen heterocycles can be used as valuable intermediates for the preparation of dye stuffs [34] and pharmaceutical products [35–37] since they exhibit a wide range of biological activities. Nanda et al. [38] reported the antibacterial activity and QSAR studies of some 3-{arylideneamino}-2-phenyl quinazoline-4(3*H*)-ones. The three dimensional quantitative structure activity relation (QSAR) studies for one large set of quinazoline type epidermal growth factor receptor (EGF-R) inhibitors were conducted using two types of molecular field analysis techniques: comparative molecular field analysis and comparative molecular similarity indices analysis [39]. A number of reports have shown that a broad class of 4-anilinoquinazolines are potent and highly selective inhibitors of EGF-R phosphorylation [4,5,42,40,41]. Chen et al. [42] reported the intramolecular imidate-amide rearrangement of 2-substituted 4-(chloroalkoxy)quinazoline derivatives. Quantum mechanical study of the competitive hydration between protonated quinazoline and Li^+, Na^+ and Ca^{2+} ions are reported by Sawunyama et al. [43]. Various quinazoline derivatives interrupted pregnancy by 40–50% and shows anti-implantation activity and also used in contraceptive compositions [44]. The present study is on the analysis of FT-IR and FT-Raman spectra of 3-amino-2-phenyl quinazolin-4(3*H*)-one and using the computational method, theoretically the wavenumbers were calculated. This work is a part of our investigations of substituted quinazoline derivatives. The authors have reported the spectroscopic studies of 3-{[(2-hydroxyphenyl)methylene]amino}-2-phenylquinazolin-4(3*H*)-one [45] and 3-{[(4-fluorophenyl)methylene]-2-phenylquinazolin-4(3*H*)-one [46].

2. Experimental

To an ethanolic solution of 2-phenyl-3,1-benzoxazin-4(3*H*)-one (1 g, 4.22 mmole) hydrazine hydrate (98%, 1.5 ml) was added and the mixture was heated in a water bath for about 3 h. The flask containing the reaction mixture was cooled and the solid thus formed was filtered and washed with water. The air dried product was re-crystallized from ethanol. Purity of the compound was checked by thin layer chromatography, using benzene and ethyl acetate as mobile phase in the ration 7:3. Iodine vapour was used as detecting agent. Yield was found to be 87%. Melting point was determined in open capillary tubes on a Thomas Hoover apparatus and was uncorrected. m.p. 177–180 °C. Mass spectra recorded on a FAB, JOEL SX 102 mass spectrometer and NMR spectra were recorded on a Bruker-Avance 300 MHz FT-NMR spectrometer, solvent $CDCl_3$, TMS internal standard, the peak assignments—were done on the basis of TOCSY, COSY and HSQC(HETCORR) spectra in addition to ^{13}C-spectra; the assigned proton shifts δ (ppm): H8, 8.33, H10, 7.78, H7, 7.78, H9, 7.52, H15,17, 7.78, H19,20, 7.52, N–H–H bonded, 5.02, N–H free, 1.7; the assigned ^{13}C shifts δ (ppm): C4, 126.39, C5, 129.24, C6, 134.5, C1, 130.2, C12,13, 129.25, C14,16, 129.25, C18, 127.06, C22, 161.6, C3, 120.1, C2, 146.99, C23, 154.6, C11, 134.05. Proton coupling values in Hz: J8,9, 8.2, J8,10, 1.0, J9,10, 0.0; The other coupling values are not calculated due to close super imposition of the protons. MS(*m*/*z*) 238(M + 1), 223(M-14). Anal. Calculated/found: H 4.67/4.63, C 70.87/70.91, N17.71/17.69.

The FT-IR spectrum (Fig. 1) was recorded on a DR/Jasco FT-IR spectrometer with KBr pellets. The FT-Raman spectrum (Fig. 2) was obtained on a Bruker RFS 100/s, Germany. For excitation of the spectrum the emission of Nd:YAG laser was used, excitation wavelength 1064 nm, maximal power 150 mW, resolution 2 cm^{-1}, measurement on solid sample.

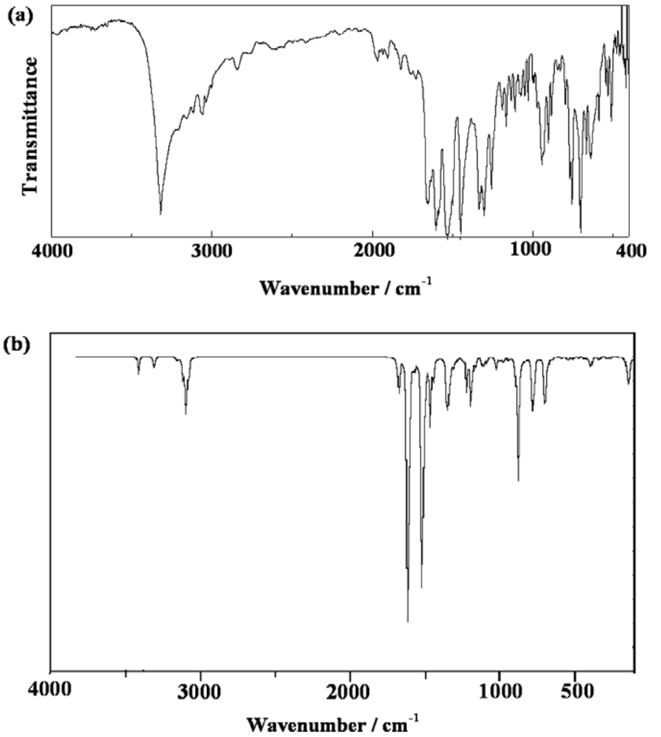

Fig. 1. FT-IR spectrum of 3-amino-2-phenyl quinazolin-4(3*H*)-one (a) experimental (b) theoretical – B3LYP.

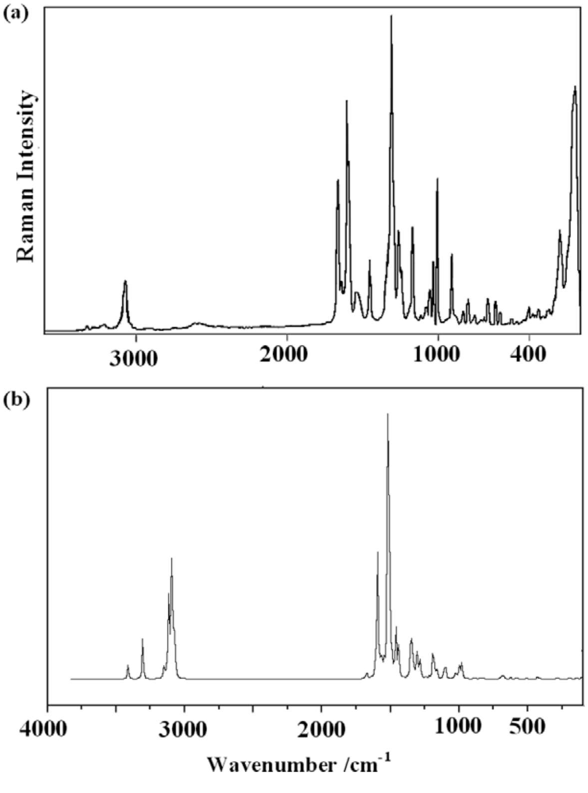

Fig. 2. FT-Raman spectrum of 3-amino-2-phenyl quinazolin-4(3*H*)-one (a) experimental (b) theoretical – B3LYP.

3. Computational details

Calculations of the title compound were carried out with Gaussian03 software program [47] using the HF/6-31G* and B3LYP/6-31G* basis sets to predict the molecular structure and vibrational wavenumbers. Calculations were carried out with Becke's three parameter hybrid model using the Lee–Yang–Parr correlation functional (B3LYP) method. Molecular geometries were fully optimized by Berny's optimization algorithm using redundant internal coordinates. Harmonic vibrational wavenumbers were calculated using analytic second derivatives to confirm the convergence to minima on the potential surface. At the optimized structure (Fig. 3) of the examined species, no imaginary wavenumber modes were obtained, proving that a true minimum on the potential surface was found. The DFT hybrid B3LYP functional tends also to overestimate the fundamental modes; therefore scaling factors have to be used for obtaining a considerably better agreement with experimental data. Therefore, a scaling factor of 0.9613 and 0.8929 were uniformly applied to the B3LYP and HF calculated wavenumbers [48]. The observed disagreement between theory and experiment could be a consequence of the anharmonicity and of the general tendency of the quantum chemical methods to overestimate the force constants at the exact equilibrium geometry. The potential energy distribution (PED) is calculated with the help of GAR2PED software package [49]. Parameters corresponding to optimized geometry (DFT) of the title compound are given in Table 1.

4. Results and discussion

The observed IR and Raman bands with their relative intensities and calculated (scaled) wavenumbers and assignments are given in Table 2.

4.1. IR and Raman spectra

In N- or S-bonded NH_2, the asymmetric NH_2 stretching vibration is observed at $3350 \pm 40\ cm^{-1}$ as in hydrazine [50–52], thiosemicarbazides [53,54], *N*-aminoheretocyclic aromatic compounds [55] and sulfonamides [56–59] and the NH_2 symmetric stretching vibration [60] in the region $3250 \pm 70\ cm^{-1}$. In the present case the DFT calculations give values 3414 and $3306\ cm^{-1}$ as asymmetric and symmetric NH_2 stretching modes. The NH_2 scissoring vibration give rise to a band in the region $1620 \pm 20\ cm^{-1}$ and the rocking vibration [60] in the range $1195 \pm 90\ cm^{-1}$. The NH_2 scissoring vibrations are observed at $1647\ cm^{-1}$ in IR spectrum, $1636\ cm^{-1}$

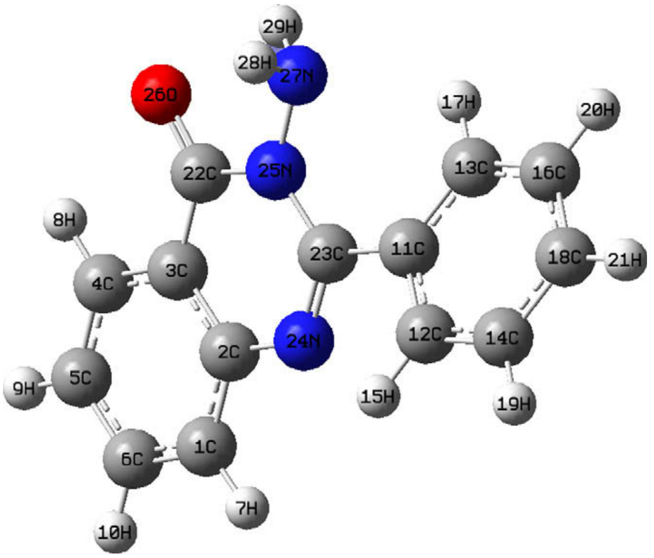

Fig. 3. Optimized geometry of 3-amino-2-phenyl quinazolin-4(3*H*)-one.

Table 1
Optimized geometrical parameters (DFT) of 3-amino-2-phenyl quinazolin-4(3*H*)-one, atom labeling is according to Fig. 3.

Bond lengths (Å)	Bond angles (°)	Dihedral angles (°)
$C_1{-}C_2$ 1.4115	$A(2,1,6)$ 120.0	$D(6,1,2,3)$ −0.0
$C_1{-}C_6$ 1.3882	$A(2,1,7)$ 118.0	$D(6,1,2,24)$ −179.2
$C_1{-}H_7$ 1.0836	$A(6,1,7)$ 122.0	$D(7,1,2,3)$ 179.7
$C_2{-}C_3$ 1.4164	$A(1,2,3)$ 119.1	$D(7,1,2,24)$ 0.6
$C_2{-}N_{24}$ 1.3892	$A(1,2,24)$ 119.0	$D(2,1,6,5)$ 0.1
$C_3{-}C_4$ 1.4081	$A(3,2,24)$ 121.9	$D(2,1,6,10)$ 179.9
$C_3{-}C_{22}$ 1.4513	$A(2,3,4)$ 120.4	$D(7,1,6,5)$ −179.7
$C_4{-}C_5$ 1.3887	$A(2,3,22)$ 118.7	$D(7,1,6,10)$ 0.2
$C_4{-}H_8$ 1.0841	$A(4,3,22)$ 120.8	$D(1,2,3,4)$ −0.1
$C_5{-}C_6$ 1.4126	$A(3,4,5)$ 119.7	$D(1,2,3,22)$ 178.6
$C_5{-}H_9$ 1.0847	$A(3,4,8)$ 118.6	$D(24,2,3,4)$ 179.1
$C_6{-}H_{10}$ 1.0853	$A(5,4,8)$ 121.7	$D(24,2,3,22)$ −2.3
$C_{11}{-}C_{12}$ 1.4103	$A(4,5,6)$ 120.1	$D(1,2,24,23)$ 179.7
$C_{11}{-}C_{13}$ 1.4092	$A(4,5,9)$ 120.1	$D(3,2,24,23)$ 0.6
$C_{11}{-}C_{23}$ 1.4873	$A(6,5,9)$ 119.8	$D(2,3,4,5)$ 0.1
$C_{12}{-}C_{14}$ 1.3949	$A(1,6,5)$ 120.7	$D(2,3,4,8)$ 179.9
$C_{12}{-}H_{15}$ 1.0829	$A(1,6,10)$ 119.7	$D(22,3,4,5)$ −178.5
$C_{13}{-}C_{16}$ 1.3983	$A(5,6,10)$ 119.6	$D(22,3,4,8)$ 1.3
$C_{13}{-}H_{17}$ 1.0805	$A(12,11,13)$ 118.9	$D(2,3,22,25)$ 0.8
$C_{14}{-}C_{18}$ 1.4006	$A(12,11,23)$ 116.9	$D(2,3,22,26)$ −179.5
$C_{14}{-}H_{19}$ 1.0853	$A(13,11,23)$ 124.1	$D(4,3,22,25)$ 179.4
$C_{16}{-}C_{18}$ 1.3990	$A(11,12,14)$ 120.7	$D(4,3,22,26)$ -0.9
$C_{16}{-}H_{20}$ 1.0854	$A(11,12,15)$ 118.5	$D(3,4,5,6)$ 0.0
$C_{18}{-}H_{21}$ 1.0855	$A(14,12,15)$ 120.8	$D(3,4,5,9)$ −179.9
$C_{22}{-}N_{25}$ 1.4172	$A(11,13,16)$ 120.1	$D(8,4,5,6)$ −179.8
$C_{22}{-}O_{26}$ 1.2565	$A(11,13,17)$ 119.5	$D(8,4,5,9)$ 0.2
$C_{23}{-}N_{24}$ 1.3155	$A(16,13,17)$ 120.3	$D(4,5,6,1)$ −0.1
$C_{23}{-}N_{25}$ 1.3996	$A(12,14,18)$ 120.1	$D(4,5,6,10)$ −179.9
$N_{25}{-}N_{27}$ 1.4254	$A(12,14,19)$ 119.7	$D(9,5,6,1)$ 179.9
$N_{27}{-}H_{28}$ 1.0201	$A(18,14,19)$ 120.2	$D(9,5,6,10)$ −0.0
$N_{27}{-}H_{29}$ 1.0214	$A(13,16,18)$ 120.6	$D(13,11,12,14)$ 1.2
	$A(13,16,20)$ 119.4	$D(13,11,12,15)$ −178.0
	$A(18,16,20)$ 120.0	$D(23,11,12,14)$ 177.1
	$A(14,18,16)$ 119.6	$D(23,11,12,15)$ −2.2
	$A(14,18,21)$ 120.2	$D(12,11,13,16)$ −0.5
	$A(16,18,21)$ 120.2	$D(12,11,13,17)$ −179.9
	$A(3,22,25)$ 115.0	$D(23,11,13,16)$ −176.0
	$A(3,22,26)$ 126.0	$D(23,11,13,17)$ 4.6
	$A(25,22,26)$ 119.0	$D(12,11,23,24)$ −28.09
	$A(11,23,24)$ 117.5	$D(12,11,23,25)$ 150.1
	$A(11,23,25)$ 121.8	$D(13,11,23,24)$ 147.5
	$A(24,23,25)$ 120.7	$D(13,11,23,25)$ −34.3
	$A(2,24,23)$ 120.3	$D(11,12,14,18)$ −1.0
	$A(22,25,23)$ 123.2	$D(11,12,14,19)$ 179.3
	$A(22,25,27)$ 115.2	$D(15,12,14,18)$ 178.3
	$A(23,25,27)$ 121.5	$D(15,12,14,19)$ −1.5
	$A(25,27,28)$ 110.0	$D(11,13,16,18)$ −0.5
	$A(25,27,29)$ 106.17	$D(11,13,16,20)$ 179.4
	$A(28,27,29)$ 111.1	$D(17,13,16,18)$ 178.9
		$D(17,13,16,20)$ −1.1
		$D(12,14,18,16)$ −0.0
		$D(12,14,18,21)$ −179.8
		$D(19,14,18,16)$ 179.7
		$D(19,14,18,21)$ −0.1
		$D(13,16,18,14)$ 0.8
		$D(13,16,18,21)$ −179.4
		$D(20,16,18,14)$ −179.2
		$D(20,16,18,21)$ 0.6
		$D(3,22,25,23)$ 2.4
		$D(3,22,25,27)$ −178.8
		$D(26,22,25,23)$ −177.3
		$D(26,22,25,27)$ 1.5
		$D(11,23,24,2)$ −179.2
		$D(25,23,24,2)$ 2.7
		$D(11,23,25,22)$ 177.6
		$D(11,23,25,27)$ −1.1
		$D(24,23,25,22)$ −4.3
		$D(24,23,25,27)$ 177.0
		$D(22,25,27,28)$ 102.4
		$D(22,25,27,29)$ −17.9
		$D(23,25,27,28)$ −78.8
		$D(23,25,27,29)$ 160.9

Table 2
Calculated vibrational wavenumbers (scaled), measured infrared and Raman band positions and assignments for 3-amino-2-phenyl quinazolin-4(3*H*)-one.

$\upsilon_{(HF)}$ (cm^{-1})	IR intensity	Raman activity	$\upsilon_{(DFT)}$ (cm^{-1})	IR intensity	Raman activity	$\upsilon_{(IR)}$ (cm^{-1})	$\upsilon_{(Raman)}$ (cm^{-1})	Assignments of normal modes with PED (%)[a]
3457	9.47	45.85	3414	18.55	55.31			$\upsilon_{as}NH_2$ (99)
3363	1.85	94.55	3306	10.87	152.98	3318 vs	3318 w	$\upsilon_{s}NH_2$ (100)
3047	8.07	131.70	3150	5.30	54.52	3143 w		$\upsilon C_{13}H_{17}$ (98)
3036	11.94	114.60	3121	5.37	58.06	3125 w		$\upsilon C_{12}H_{15}$ (93)
3034	10.18	203.45	3115	15.32	241.82			υC_1H_7 (57), υC_4H_8 (20), υC_6H_{10} (12), υC_5H_9 (10)
3027	30.07	123.94	3110	8.89	63.87			υC_4H_8 (58), υC_1H_7 (31), υC_5H_9 (10)
3021	24.74	160.91	3096	39.88	268.10			$\upsilon C_{18}H_{21}$ (54), $\upsilon C_{14}H_{19}$ (21), $\upsilon C_{16}H_{20}$ (21)
3017	22.12	92.79	3094	16.86	162.01			υC_5H_9 (48), υC_6H_{10} (25), υC_4H_8 (18)
3006	1.53	87.92	3081	22.33	133.04			$\upsilon C_{14}H_{19}$ (50), $\upsilon C_{16}H_{20}$ (46)
3005	7.89	77.36	3079	5.78	78.46			υC_6H_{10} (61), υC_5H_9 (31)
2998	6.03	30.43	3070	0.34	60.32	3050 w	3070 s	$\upsilon C_{18}H_{21}$ (45), $\upsilon C_{16}H_{20}$ (31), $\upsilon C_{14}H_{19}$ (22)
1772	553.04	23.87	1675	42.48	24.15	1658 s	1660 vs	$\upsilon C_{22}O_{26}$ (63)
1669	302.99	246.26	1614	271.22	13.21	1647 sh	1636 w	δNH (82), υC_3C_{22} (13)
1640	138.16	166.49	1605	73.24	40.96	1603 vs	1601 vvs	υPh I (55), δCCC I (11)
1621	131.56	83.76	1594	2.03	499.47		1584 h	υPh II (54), δCCC II (10), δCH II (16)
1615	25.56	64.74	1571	14.66	88.81			υPh II (61), δCH II (11)
1589	8.35	8.21	1551	1.27	72.31			υPh I (67), δCCC I (10), δCH I (15)
1550	48.82	124.40	1515	360.95	1521.11	1534 vvs	1538 m	$\upsilon C_{23}N_{24}$ (64)
1493	26.35	0.99	1489	14.03	71.56	1490 sh		δCH II (59), υPh II (30)
1474	91.49	32.61	1463	55.58	78.60	1466 m		δCH I (44), υPh I (29)
1455	12.13	0.71	1462	21.86	113.38			δCH I (43), υPh I (19)
1438	12.33	2.85	1443	22.24	121.33	1449 vvs	1449 s	δCH II (50), υPh II (22)
1346	95.32	66.83	1351	66.03	190.58			$\upsilon C_{23}N_{25}$ (28), $\gamma N_{25}H_{28}H_{29}N_{27}$ (24), $\delta C_{22}N_{27}N_{25}$ (12)
1314	8.32	8.00	1343	32.39	90.18			υPh I (68)
1313	13.19	24.04	1333	21.95	31.85			δCH II (38), υPh II (12), υPh I (11)
1288	25.40	9.82	1318	4.42	6.91	1315 s		υPh II (66)
1276	100.54	17.30	1306	11.59	105.78	1307 s	1304 vvs	δNH (64)
1238	6.69	77.38	1285	4.97	92.41	1284 m		δNH (22), $\upsilon C_{23}N_{25}$ (11), δCH I (10), υPh II (11)
1208	29.08	16.80	1245	4.40	10.27	1258 m	1258 m	υC_2N_{24} (28), υPh I (14), $\upsilon C_{11}C_{23}$ (25)
1193	2.85	0.79	1220	36.76	10.79		1239 m	υC_3C_{22} (13), δCCC I (10), δCH I (15), $\upsilon C_{23}N_{24}$ (10), $\upsilon C_{22}N_{25}$ (10)
1182	0.96	17.83	1193	15.62	8.42			δCH II (75), υPh II (14)
1163	2.00	3.93	1188	60.94	152.90	1180 w		$\upsilon N_{25}N_{27}$ (39), δCH I (28)
1131	12.68	42.12	1176	0.21	11.70			δCH II (86)
1098	24.96	2.57	1163	8.96	29.07	1166 w	1165 s	δCH I (70)
1088	6.63	7.21	1111	16.05	44.06	1140 m		$\upsilon C_{22}N_{25}$ (15), υPh I (16), δCH I (24)
1083	4.01	12.30	1099	1.93	56.93	1110 w	1108 w	$\upsilon C_{22}N_{25}$ (52), δCCC I (22)
1056	1.32	0.32	1084	7.41	0.62	1080 w	1079 w	υPh II (48), δCH II (31)
1013	1.37	20.29	1030	4.77	19.02	1029 w	1050 m	υPh II (51), δCCC II (11)
1011	1.79	2.95	1020	12.55	13.10	1015 w	1029 s	υPh I (55), δCH I (21)
1010	0.20	0.69	1000	3.17	44.79		1002 vs	δCCC II (61)
1009	2.01	0.90	999	0.01	0.51			γCH I (85), τCCCC I (13)
988	0.75	0.17	998	0.26	1.54	995 w		γCH II (79), τCCCC II (18)
988	1.84	0.09	983	3.80	76.45			$\upsilon C_{22}N_{25}$ (12), υPh II (22), $\delta CN_{27}N_{25}$ (16)
976	1.53	3.96	975	2.89	3.71			γCH II (86)
971	19.36	54.99	971	2.08	0.25			γCH I (90)
949	88.94	1.75	940	3.49	2.56	943 m		γCH II (83)
930	121.68	2.22	891	19.37	5.401	903 m	904 s	δCCC I (39), δQRing (10), $\delta NC_{11}C_{23}$ (16)
891	4.67	3.20	888	1.76	3.65			γCH I (79)
861	11.33	4.18	875	128.07	1.92	853 w		$\gamma N_{25}H_{28}H_{29}N_{27}$ (57), $\upsilon N_{25}N_{27}$ (14)
852	62.02	2.38	850	5.17	7.38			γCH II(98)
811	33.59	2.28	831	3.51	6.81	826 w	826 w	$\upsilon N_{25}N_{27}$ (10), υPh I (20), δCCC I (14)
799	5.42	1.22	794	1.63	1.68	792 w	798 w	τQRing (29), $\gamma O_{26}C_3N_{25}C_{22}$ (22), τCCCC I (19)
783	48.47	0.22	782	3.91	0.12			τCCCC II (20), γCH II (15), $\gamma C_{23}C_{12}C_{13}C_{11}$ (14)
774	78.01	0.59	775	82.29	0.75	755 s	758 w	γCH I (52), τCCCC I (15), τQRing (12)
716	10.85	2.94	698	75.01	2.90	702 vs		τCCCC I (15), $\gamma C_{11}N_{25}N_{24}C_{23}$ (13), γCH II (27), τCCCC II (11)
698	40.96	3.23	692	8.53	2.58			τCCCC II (35), τCCCC I (17), γCH II (11)
696	17.49	1.92	687	11.13	12.66		688 w	τCCCC II (19), $\upsilon N_{25}N_{27}$ (14), δCCC I (19), δQRing (16)
686	2.88	6.49	680	0.97	4.81			$\gamma O_{26}C_3N_{25}C_{22}$ (23), $\gamma C_{11}N_{25}N_{24}C_{23}$ (17), τCCCC II (14), τQRing (13)
659	6.14	7.73	673	3.58	9.36	666 m	666 m	δCCC II (40), δCCC I (18), δQRing (18)
635	17.41	0.45	649	3.82	0.27	638 m		δCCC I (17), $\delta C_3O_{26}C_{22}$ (15), $\delta N_{25}O_{26}C_{22}$ (15), $\delta NC_{11}C_{23}$ (14), $\delta CN_{27}N_{25}$ (10)
604	0.11	6.03	626	0.13	6.88		618 w	δCCC II (81)
568	2.53	2.41	583	1.51	7.75	569 w	587 w	δCCC I (44), δQRing (19), δCCC II (12)
540	5.55	0.47	543	6.68	1.31	531 w		τCCCC I (41), τQRing (15), γCH I (15)
503	4.95	6.09	512	3.67	6.42	511 w	511 w	δQRing (54), δCCC I (10)
485	6.04	0.51	473	1.72	1.07	470 w	480 w	τCCCC II (35), $\gamma C_{23}C_{12}C_{13}C_{11}$ (20), τCCCC I (10)
438	0.03	0.20	445	0.23	0.42	440 w		τCCCC I (54), $\tau C_4C_3C_2N_{24}$ (16), $\tau C_{22}C_3C_2C_1$ (16)
419	2.29	7.71	430	2.64	11.95	425 w		δQRing (51) , υC_3C_{22} (13)
406	0.29	1.96	410	3.86	4.29	419 w		τCCCC II (78)
385	4.94	1.83	390	17.51	2.62		396 w	$\delta CN_{27}N_{25}$ (35), $\delta C_3O_{26}C_{22}$ (22), τCCCC II (18)
338	2.48	3.03	334	4.23	2.35		333 w	$\delta CC_{23}C_{11}$ (28), τCCCC I (17), $\delta CN_{27}N_{25}$ (20)
298	5.14	0.91	301	0.13	1.06			τCCCC II (15), τCCCC I (16), δQRing (32)

Table 2 (*continued*)

$\upsilon_{(HF)}$ (cm^{-1})	IR intensity	Raman activity	$\upsilon_{(DFT)}$ (cm^{-1})	IR intensity	Raman activity	$\upsilon_{(IR)}$ (cm^{-1})	$\upsilon_{(Raman)}$ (cm^{-1})	Assignments of normal modes with PED (%)[a]
267	2.09	4.34	284	1.49	4.29			τCCCC II (20), $\delta CC_{23}C_{11}$ (36), δQRing (30)
250	3.66	1.44	282	0.89	4.36			$\gamma N_{27}C_{22}C_{23}N_{25}$ (63), τQRing (20)
236	0.55	2.28	262	1.41	0.47		270 w	δCCC I (25), $\delta CC_{23}C_{11}$ (20), δCCC II (16)
201	7.31	3.89	197	1.10	7.64		191 s	$\tau C_4C_3C_2N_{24}$ (19), $\tau C_{22}C_3C_2C_1$ (19), τCCCC II (16), τQRing (19), $\delta CC_{23}C_{11}$ (12)
181	37.44	2.01	147	30.82	2.85			τNH(47), τCCCC I (10)
130	0.77	1.23	133	24.67	4.34			τNH(29), $\gamma N_{27}C_{22}C_{23}N_{25}$ (15), τQRing (20), τCCCC I (18)
95	4.71	5.11	110	2.00	11.20			τNH (19), τQRing (19), $\delta NC_{11}C_{23}$ (16), $\delta CN_{27}N_{25}$ (12)
71	2.04	2.83	90	10.33	1.71		90 vs	τQRing (41), $\delta NC_{11}C_{23}$ (13), τNH2 (10)
52	0.09	2.80	51	0.04	1.33			τQRing (42), $\gamma C_{11}N_{25}N_{24}C_{23}$ (18), $\gamma C_{23}C_{12}C_{13}C_{11}$ (13)
31	0.14	11.99	38	0.12	8.16			$\tau CCC_{23}N$ (65), $\delta NC_{11}C_{23}$ (16), $\delta CC_{23}C_{11}$ (14)

υ, stretching; δ, in-plane bending; γ, out-of-plane bending; τ, torsion; s, strong; m, medium; w, weak; v, very; br, broad; ortho and mono substituted phenyl rings are designated as PhI and PhII; QRing, quinazoline ring.

[a] PED, potential energy distribution, only contribution larger than 10% were given.

in Raman spectrum and at 1614 cm^{-1} theoretically. The band observed at 1307 cm^{-1} in the IR spectrum and 1304 cm^{-1} in the Raman spectrum is assigned as the rocking mode of NH_2 group. The DFT calculation gives this mode at 1306 cm^{-1}. The wagging vibration is expected in the region 830 ± 50 cm^{-1} and torsion [60] in the region 280 ± 70 cm^{-1}. The DFT calculations give the wagging mode of NH_2 at 875 cm^{-1}. For the title compound the torsional modes of NH_2 are below 400 cm^{-1}. Sundaraganesan et al. [61] reported NH_2 vibrations at 1632, 1284, 1223 cm^{-1} (IR) and 1280, 987 cm^{-1} (Raman).

The carbonyl group is contained in a large number of different classes of compounds, for which a strong absorption band due to the C=O stretching vibration is observed in the region [62] 1850–1550 cm^{-1}. If a carbonyl group is part of a conjugated system, then the wavenumber of the carbonyl stretching vibration decreases, the reason being that the double bond character of the C=O group is less due to the π-electron conjugation being localized. For the title compound, the υC=O mode is seen as a strong band at 1658 cm^{-1} in the IR and at 1660 cm^{-1} in the Raman spectrum. The DFT calculations give this mode at 1675 cm^{-1}. But the electron-releasing effect in the C=O double bond causes a polarizability change during vibration, making the Raman band intensity comparable to that of the IR band. Also, here the intra molecular charge transfer takes place via a conjugated phenyl ring path which makes the phenyl ring stretching mode at 1603 (IR), 1601 cm^{-1} (Raman) simultaneously active in the IR and Raman spectra [63]. The deformation bands of C=O group are also identified (Table 2).

The C=N stretching skeletal bands [64–66] are observed in the range 1650–1500 cm^{-1}. For conjugated azines, the υC=N mode is reported [67] at 1553 cm^{-1}. For the title compound the band observed at 1534 cm^{-1} in the IR spectrum and at 1538 cm^{-1} in the Raman spectrum is assigned as υC=N mode. The B3LYP calculations give this mode at 1515 cm^{-1}.

Corresponding to =C–N stretching vibration [62], two bands are observed in the regions 1360–1250 and 1280–1180 cm^{-1} for aromatic and unsaturated amines. Primary and secondary aromatic amines absorb strongly in the first region. Primary aromatic amines with nitrogen directly on the ring absorb at 1330–1260 cm^{-1} because of the stretching of the phenyl C–N bond [68]. The C=N stretching bands are reported in the range [69] 1100–1300 cm^{-1}. In the present case, the $\upsilon C_2–N_{24}$ mode is observed at 1258 (IR), 1258 (Raman), 1245 (DFT), $\upsilon C_{23}–N_{25}$ mode at 1351 (DFT) and $\upsilon C_{22}–N_{25}$ mode at 1108 (IR), 1110 cm^{-1} (Raman). These modes are not pure but contain significant contributions from other modes. υN–N has been reported at 1115 cm^{-1} by Crane et al. [70], at 1121 cm^{-1} by Bezerra et al. [71] and at 1130 cm^{-1} by El-Behery and El-Twigry [72]. Sundaraganesan et al. [61] reported the υN–N stretching mode at 1083 cm^{-1} theoretically. The DFT calculations give this υN–N mode at 1188 cm^{-1} in the present case and a weak band is observed at 1180 cm^{-1} in the IR spectrum.

The existence of one or more aromatic ring in a structure is normally readily determined from the C–H and C=C–C related vibrations. The C–H stretching occurs above 3000 cm^{-1} and is typically exhibited as a multiplicity of weak to moderate bands, compared with the aliphatic C–H stretch [73] . In the present case, the DFT calculations give the υCH modes in the range 3150–3070 cm^{-1}. The bands observed at 3143, 3125, 3050 cm^{-1} in the IR spectrum and at 3070 cm^{-1} in the Raman spectrum were assigned as υCH modes of the benzene rings.

The benzene ring possesses six ring stretching vibrations, of which the four with the highest wavenumbers (occurring near 1600, 1580, 1490 and 1440 cm^{-1}) are good group vibrations. In the absence of ring conjugation, the band near 1580 cm^{-1} is usually weaker than that at 1600 cm^{-1}. The fifth ring stretching vibration which is active near 1335 ± 35 cm^{-1} a region which overlaps strongly with that of the CH in-plane deformation and the intensity is in general, low or medium high [60]. The sixth ring stretching vibration or ring breathing mode appears as a weak band near 1000 cm^{-1} in mono, 1,3-di and 1,3,5-trisubstituted benzenes. In the other wise substituted benzene, however, this vibration is substituent sensitive and difficult to distinguish from the ring in-plane deformation.

In the following discussion, the mono and ortho substituted phenyl rings are designated as rings II and I, respectively. The modes in the two phenyl rings will differ in wavenumber and the magnitude of splitting will depend on the strength of interactions between different parts (internal coordinates) of the two rings. For some modes, this splitting is so small that they may be considered as quasi-degenerate and for the other modes a significant amount of splitting is observed. Such observations have already been reported [74–77].

For mono substituted benzene, the υPh modes are expected in the range of 1285–1610 cm^{-1} and for the ortho disubstituted benzene [60] these modes are seen in the region 1620–1260 cm^{-1}. The υPh modes are observed at 1603, 1534, 1466 cm^{-1} in the IR spectrum, 1601 cm^{-1} in the Raman spectrum, 1605, 1551, 1463, 1462, 1343 cm^{-1} theoretically for ring Ph I and at 1490, 1449, 1315 cm^{-1} in the IR spectrum, 1584 cm^{-1} in the Raman spectrum, 1594, 1571, 1489, 1443, 1318 cm^{-1} theoretically for ring Ph II. Due to aromatic ring vibrations, quinazolines [62] absorb strongly at 1635–1610, 1580–1565, and 1520–1475 cm^{-1}. In ortho disubstitution, the ring breathing mode has three wavenumber intervals depending on whether both substituents are heavy; or one of them is heavy, while the other is light; or both of them are light. In the first case, the interval is 1100–1130 cm^{-1}; in the second case 1020–1070 cm^{-1}; while in the third case it is between [56] 630 and 780 cm^{-1}. The ring breathing modes of the phenyl rings are assigned at 1020 cm^{-1} for ring Ph I and at 983 cm^{-1} for ring Ph II by PED calculations.

The in-plane CH vibrations are expected in the range of 1015–1300, 1010–1300 cm^{-1} for mono and ortho substituted benzenes, respectively [60]. Generally, the CH out-of-plane deformations with the highest wavenumbers have a smaller intensity than those absorbing at lower wavenumbers. Most of the deformation bands of the CH vibrations of the phenyl rings are not pure but contain significant contributions for other modes (Table 2). The out-of-plane CH deformation at 702 cm^{-1} and the in-plane ring deformation at 666 cm^{-1} form a pair of strong bands characteristics of mono substituted benzene derivatives [78]. In the case of 1,2-di substitution only one strong absorption in the region 755 ± 35 cm^{-1} is observed and is due to γCH. This band is observed at 755 cm^{-1} in the IR spectrum as a strong band for the title compound. The IR bands in the 1750–2839 cm^{-1} region and their large broadening support the intramolecular hydrogen bonding [46].

4.2. Geometrical parameters and first hyper polarizability

To best of our knowledge, no X-ray crystallographic data of this molecule have yet been established. However, the theoretical results (DFT) obtained are almost comparable with the reported structural parameters of the parent quinazoline molecules. The experimental N–N bond length of hydrazine [79] is reported at 1.449 Å and the electron diffraction N–N bond length of tetramethylhydrazine [80] is reported at 1.401 Å. Kostava et al. [81] calculated the N_{25}–N_{27} bond length in the range 1.318–1.357 Å for different molecules. In the present case the N_{25}–N_{27} bond length is 1.4254 Å which is some where between the length of an N–N single bond (1.45 Å) and an N=N double bond (1.25 Å). For the title compound, the bonds C_{23}=N_{24}=1.3155, C_{22}–O_{26} = 1.2565 Å show typical double bond characteristics. However, C_2–N_{24} = 1.3892 Å, C_{22}–N_{25} = 1.4172 Å, C_{23}–N_{25} = 1.3996 Å bond length are shorter than the normal C–N single bond length of about 1.48 Å. The shortening of the C–N bonds reveal the effects of resonance in this part of the molecule [82]. The difference between the lengths of C–N bonds is similar to the values of reported quinazoline derivatives [83] and this situation can be attributed to the difference in hybridization of the different carbon atoms. For a quinazoline derivative, Costa et al. [34] reported C_2–N_{24} = 1.3954, C_{23}–N_{25} = 1.3904 and C_{22}–N_{25} = 1.4174 Å . Gai et al. [87] reported C_{22}–N_{25}, C_{23}–N_{25}, C_2–N_{24}, C_3–C_{22} and C_2–C_3 as 1.3703, 1.4623, 1.4043, 1.4823 and 1.3903 Å, respectively for a quinazoline derivative. In the present case, the corresponding values are 1.4172, 1.3996, 1.3892, 1.4519 and 1.4164 Å, respectively. For the title compound, the DFT calculations give the bond angles C_{22}–N_{25}–N_{27} = 115.2, C_{22}–N_{25}–C_{23} = 123.2, N_{27}–N_{25}–C_{23} = 121.5, O_{26}–C_{22}–N_{25} = 119.0, O_{26}–C_{22}–C_3 = 126.0, N_{25}–C_{22}–C_3 = 115.0, C_2–C_3–C_4 = 120.4, C_2–C_3–C_{22} = 118.7, C_4–C_3–C_{22} = 120.8, C_3–C_2–C_1 = 119.1, C_3–C_2–N_{24} = 121.9, C_1–C_2–N_{24} = 119.0° where as the corresponding reported values [84] are 120.3, 121.0, 118.0, 121.8, 122.7, 115.5, 119.7, 120.6, 119.6, 120.0, 121.2 and 118.6.

For the title compound, the dihedral angles C_4–C_3–C_{22}–N_{25} = 179.4° and C_{22}–N_{25}–C_{23}–C_{11} = 177.6°. This indicates that the phenyl ring I and the quinazoline moiety of the title compound are in tilted positions. Also the dihedral angles C_{16}–C_{13}–C_{11}–C_{23}, C_{11}–C_{23}–N_{24}–C_2, and C_{11}–C_{23}–N_{25}–C_{22} are −176.0°, −179.2° and 177.6°, respectively, which shows the phenyl ring II and the quinazoline moiety are in different planes. The N_{24}–C_{23} ring moiety is slightly twisted from the phenyl ring I (C_3–C_2–N_{24}–C_{23} = 0.6° and C_1–C_2–N_{24}–C_{23} = 179.7°) and is more twisted from the phenyl ring II (N_{24}–C_{23}–C_{11}–C_{13} = 147.5° and N_{24}–C_{23}–C_{11}–C_{12} = −28.1°) as is evident from the torsion angles.

For a quinazoline derivative, Krishnakumar and Muthunatesan [85] reported the bond lengths N_{24}–C_{23}, C_{23}–N_{25}, C_{22}–C_3, C_3–C_4, C_4–C_5, C_5–C_6, C_6–C_1, C_1–C_2 as 1.311, 1.362, 1.427, 1.414, 1.380, 1.415, 1.380, 1.416 Å . In the present study the corresponding values are 1.3155, 1.3996, 1.4513, 1.4081, 1.3887, 1.4126, 1.3882, 1.4115 Å. The DFT calculations give the bond angles N_{24}–C_{23}–N_{25}, C_{23}–N_{25}–C_{22}, N_{25}–C_{22}–C_3, C_{22}–C_3–C_4, C_3–C_4–C_5, C_4–C_5–C_6, C_5–C_6–C_1, C_6–C_1–C_2 as 120.7°, 123.2°, 115.0°, 120.8°, 119.7°, 120.1°, 120.7°, 120.0°, respectively, where as the corresponding reported values are 127.7°, 123.4°, 116.2°, 124.4°, 119.5°, 120.3°, 120.9° and 120.1°, respectively [85]. Sundaraganesan et al. [61] reported the bond lengths N_{25}–N_{27} = 1.403, N_{27}–H_{28} = 1.018, N_{27}–H_{29} = 1.018 Å and bond angles N_{25}–N_{27}–H_{29} = 109.2, N_{25}–N_{27}–H_{28} = 109.2, H_{29}–N_{27}–H_{28} = 108.4. For the title compound, the corresponding values are 1.4254, 1.0201, 1.0214 Å and 106.2°, 110.0°, 111.1°.

The three bond angles around C_{22} atom are not equal to 120 each. It is seen that the C_3–C_{22}–O_{26} (126°) is considerably greater than the angle N_{25}–C_{22}–C_3 (115°). This observation is similar to that in the structures of hydrazones reported earlier [86] which is explained as due to a decrease in the repulsion between the lone pairs present in N_{25} and O_{26} atoms. The central part of the molecule adopts a completely extended double bond conformation. It can be confirmed by the C_{22}–O_{26} bond length (1.2565 Å) which is considerably longer than the standard C=O bond length 1.21 and N_{25}–C_{22} bond length (1.4172 Å) which is shorter than the standard N–C single bond length (1.47 Å) [86].

Non-linear optics deals with the interaction of applied electromagnetic fields in various materials to generate new electromagnetic fields, altered in wavenumber, phase or other physical properties [87]. Organic molecules able to manipulate photonic signals efficiently are of importance in technologies such as optical communication, optical computing and dynamic image processing [88,89]. Phenyl substituents can increase molecular hyperpolarizability, a result that has been described as surprising [90,91]. Analysis of organic molecules having conjugated π-electron systems and large hyperpolarizability using infrared and Raman spectroscopy has evolved as a subject of research [92]. The potential application of the title compound in the field of non-linear optics demands the investigation of its structural and bonding features contributing to the hyperpolarizability enhancement, by analyzing the vibrational modes using the IR and Raman spectrum.

The first hyperpolarizability (β_0) of this novel molecular system is calculated using B3LYP/6-31G* method, based on the finite field approach. In the presence of an applied electric field, the energy of a system is a function of the electric field. First hyperpolarizability is a third rank tensor that can be described by a 3 × 3 × 3 matrix. The 27 components of the 3D matrix can be reduced to 10 components due to the Kleinman symmetry [93]. The components of β are defined as the coefficients in the Taylor series expansion of the energy in the external electric field. When the electric field is weak and homogeneous, this expansion becomes

$$E = E_0 - \sum_i \mu_i F^i - \frac{1}{2}\sum_{ij}\alpha_{ij}F^iF^j - \frac{1}{6}\sum_{ijk}\beta_{ijk}F^iF^jF^k - \frac{1}{24}\sum_{ijkl}\gamma_{ijkl}F^iF^jF^kF^l + \cdots$$

where E_0 is the energy of the unperturbed molecule, F^i is the field at the origin, μ_i, α_{ij}, β_{ijk} and γ_{ijkl} are the components of dipole moment, polarizability, the first hyper polarizabilities, and second hyperpolarizibilites, respectively. The calculated first hyperpolarizability of the title compound is 5.05 × 10^{-30} esu, which is comparable with

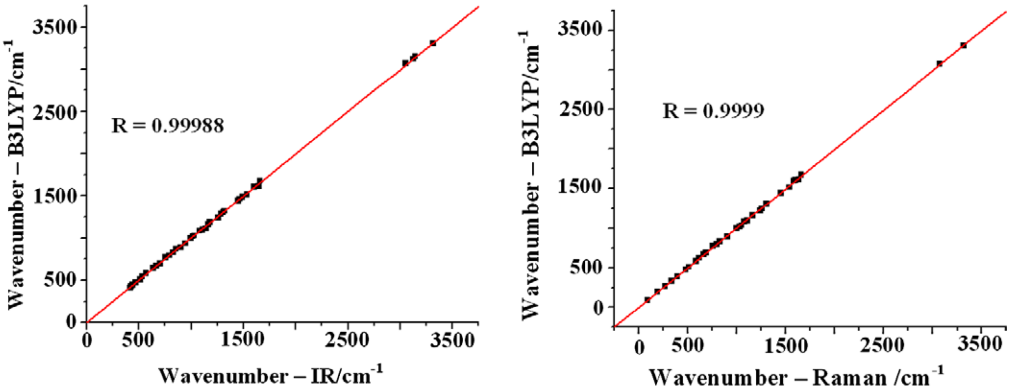

Fig. 4. Correlation graph.

the reported values of similar quinazoline derivatives [94] and experimental evaluation of this data is not readily available. The authors have reported the hyperpolarzability values 0.92×10^{-30} and 2.445×10^{-30} esu for similar quinazoline derivatives [45,46]. The C–N distances in the calculated molecular structure vary from 1.3892 to 1.4172 Å which are intermediate between those of a C–N single bond (1.48 Å) and a C=N double bond (1.28 Å). Therefore, the calculated data suggest an extended π-electron delocalization over the quinazoline moiety [95], which is responsible for the non-linearity of the molecule. We conclude that the title compound is an attractive object for future studies of non-linear optical properties.

In order to investigate the performance and vibrational wavenumbers of the title compound root mean square value (RMS) and correlation coefficient between calculated (scaled DFT) and observed wavenumbers were calculated (Fig. 4). RMS values of wavenumbers were evaluated using the following expression [96].

$$RMS = \sqrt{\frac{1}{n-1}\sum_{i}^{n}(\upsilon_i^{calc} - \upsilon_i^{exp})^2}$$

The RMS error of the observed Raman bands and IR bands are found to be 36.13 and 38.05 for HF method and 10.59 and 11.92 for DFT method. The small differences between experimental and calculated vibrational modes are observed. It must be due to the fact that hydrogen bond vibrations present in the crystal lead to strong perturbation of the infrared wavenumbers and intensities of many other modes. Also, we state that experimental results belong to solid phase and theoretical calculations belong to gaseous phase.

5. Conclusion

The FT-IR and FT-Raman spectra of 3-amino-2-phenyl quinazolin-4(3*H*)-one were studied. The molecular geometry and wavenumber have been calculated using HF/6-31G* and B3LYP/6-31G* basis and the normal modes are assigned by PED calculations. The simultaneous IR and Raman activation of the C=O stretching modes gives the charge transfer interaction through a π-conjugated path. Optimized geometrical parameters of the title compound are in agreement with the reported values. Analysis of the phenyl ring modes shows that C–C stretching mode is found equally active as strong bands in both IR and Raman, which can be interpreted as the evidence of intramolecular charge transfer via conjugated ring path, which is responsible for hyperpolarizability enhancement, leading to non-linear optical activity.

References

[1] K. Spirkova, S. Stankovsky, A. Mrvova, L. Cipak, Chem. Pap. 53 (1999) 272.
[2] M.A. Al-Omar, S.G. Abdel-Hamide, H.A. Alkhamees, H.I. El-Subbagh, Saudi Pharm. J. 12 (2004) 63.
[3] M. Zia-Ur-Rehman, J.A. Choudary, S. Ahmad, H.L. Siddiqui, Chem. Pharm. Bull. 54 (2006) 1175.
[4] D.W. Fry, A.J. Kraker, A. McMichael, L.A. Ambroso, J.M. Nelson, W.R. Leopold, R.W. Connors, A.J. Bridges, Science 265 (1994) 1093.
[5] T.M. Traxler, P. Furet, H. Mett, E. Buchdunger, T. Meyer, N. Lydon, J. Med. Chem. 39 (1996) 2285.
[6] J.H. Hynes, A. Tomazic, A. Kumar, V. Kumar, J.H. Freisheim, J. Heterocycl. Chem. 28 (1991) 1981.
[7] N.V. Harris, C. Smith, K. Bowden, J. Med. Chem. 27 (1992) 7.
[8] R.O. Dempcy, E.B. Skibo, Biochemistry 30 (1991) 8480.
[9] A.K. Sengupta, A.A. Gupta, J. Antibact, Agents 8 (1980) 7.
[10] V. Alagarsamy, U.S. Pathak, D. Sriram, S.N. Pandeya, E. De Clercq, Indian J. Pharm. Sci. 62 (2000) 433.
[11] R. Nigam, S. Swarup, V.K. Saxena, Indian Drugs 27 (1990) 238.
[12] H. Manabu, I. Ryvichi, H. Hideak, Chem. Pharm. Bull. 38 (1990) 618.
[13] J. Dowell, J.D. Minna, P. Korkpatrick, Nat. Rev. Drug Discov. 4 (2005) 514.
[14] M. Bos, J. Mondelsohn, Y.M. Kim, J. Albanell, D.W. Fry, J. Baselga, Clin. Cancer Res. 3 (1997) 2099.
[15] V. Alagarsamy, R. Giridhar, H.R. Yadav, R. Revathi, K. Rukmani, E. De Clercq, Indian J. Pharm. Sci. 68 (2006) 532.
[16] V.K. Srivastava, A. Singh, A. Gucati, K. Shankar, Indian J. Chem. 26 (1987) 652.
[17] D.P. Gupta, S. Ahmed, A. Kumar, K. Shankar, Indian J. Chem. 27 (1988) 1060.
[18] V. Jatav, P. Mishra, S. Kashaw, J.P. Stables, Eur. J. Med. Chem. 43 (2008) 135.
[19] V. Joshi, R.P. Chaurasia, Indian J. Chem. 26 (1987) 602.
[20] I.R. Prouse, Drugs Future 18 (1993) 475.
[21] S.V. Bhandari, B.J. Deshmane, S.C. Dangare, S.T. Gore, V.T. Raparti, C.V. Khachane, A.P. Sarkate, Pharmacologyonline 2 (2008) 604.
[22] A.A. Bekhit, N.S. Habbib, A. Bekhit, Boll. Chim. Farm. 140 (2001) 297.
[23] M.R. Azza, E.R. Eman, G.E. Fatma, Arch. Pharm. 337 (2004) 527.
[24] V.K. Pandey, D. Mishra, S. Sukla, Indian Drugs 31 (1994) 53.
[25] V.K. Pandey, Indian Drugs 25 (1988) 168.
[26] V.K. Pandey, M. Gupta, D. Mishra, Indian Drugs 33 (1996) 409.
[27] J.B. Jiang, D.P. Hesson, B.A. Dusak, D.L. Dexter, G.J. Kang, E. Harmel, J. Med. Chem. 33 (1990) 1721.
[28] C.M. Lin, G.J. Kang, M.C. Roach, J.B. Jian, D.P. Hesson, R.F. Luduena, E. Hamel, Mol. Pharmacol. 40 (1991) 827.
[29] V.K. Pandey, S. Tusi, Z. Tusi, R. Raghubir, M. Dixit, M.N. Joshi, Indian J. Chem. 43 (2004) 180.
[30] A. Kamal, V. Devaiah, N. Sankarajah, K.L. Reddy, Synlett 16 (2006) 2609.
[31] K.M. Kimber, L. Yonno, R. Hearlip, B. Weichman, Agent Actions 39 (1993) 677.
[32] A.J. Duplantier, J.B. Cherg, Annu. Rep. Med. Chem. 29 (1994) 73.
[33] V. Alagarsamy, V.R. Saloman, G. Vanikavith, V. Paluchamy, M.R. Chandran, A.A. Sujin, A. Thangathiruppathy, S.A. Muthulakashmi, R. Revathi, Biol. Pharm. Bull. 25 (2002) 1432.
[34] M. Costa, N.D. Ca, B. Gabriele, C. Massera, G. Salerno, M. Soliani, J. Org. Chem. 69 (2004) 2469.
[35] G.R. Madhavan, R. Chakrabarti, S.K.B. Kumar, P. Misra, R.N.V.S. Mamidi, K. Balraju, R.K. Babu, J. Suresh, B.B. Loharyb, J. Iqbal, R. Rajagopalan, Eur. J. Med. Chem. 36 (2001) 627.
[36] C. Parkanyi, D.S. Schmidt, J. Heterocycl. Chem. 37 (2000) 725.
[37] P. Owalski, M.J. Mokrosz, Z. Majka, Y. Kowalska, J. Heterocycl. Chem. 37 (2000) 187.
[38] A.K. Nanda, S. Ganguli, R. Chakraborty, Molecules 12 (2007) 2413.
[39] T. Hou, L. Zhu, L. Chen, X. Xu, J. Chem. Inf. Comput. Sci. 43 (2003) 273.
[40] G.W. Rewcastle, W.A. Denny, A.J. Bridges, H.R. Zhou, D.R. Cody, A. McMichael, D.W. Fry, J. Med. Chem. 38 (1995) 3482.

[41] A. Wissner, D.M. Berger, D.H. Boschelli, B.C. Gruver, B.D. Johnson, N. Mamuya, Y.F. Wang, B.Q. Wu, F. Ye, N. Zhang, J. Med. Chem. 43 (2000) 3244.
[42] G.S. Chen, S. Kalchar, C.W. Kuo, C.S. Chang, C.O. Usifoh, J.W. Chern, J. Org. Chem. 68 (2003) 2502.
[43] P. Sawunyama, G.W. Bailey, J. Phys. Chem. A 105 (2001) 9717.
[44] A. Chowdhury, N. Sharma, P. Sharma, N.D. Jasuja, G. Sharma, S.C. Joshi, R.V. Singh, Rasayan J. Chem. 1 (2008) 648.
[45] C.Y. Panicker, H.T. Varghese, K.R. Ambujakshan, S. Mathew, S. Ganguli, A.K. Nanda, C. Van Alsenoy, J. Raman Spectrosc., doi: 10.1002/jrs.2276.
[46] C.Y. Panicker, K.R. Ambujakshan, H.T. Varghese, S. Mathew, S. Ganguli, A.K. Nanda, C. Van Alsenoy, J. Raman Spectrosc., doi: 10.1002/jrs 2159.
[47] M.J. Frisch, G.W. Trucks, H.B. Schlegel, G.E. Scuseria, M.A. Robb, J.R. Cheeseman, J.A. Montgomery Jr., T. Vreven, K.N. Kudin, J.C. Burant, J.M. Millam, S.S. Iyengar, J. Tomasi, V. Barone, B. Mennucci, M. Cossi, G. Scalmani, N. Rega, G.A. Petersson, H. Nakatsuji, M. Hada, M. Ehara, K. Toyota, R. Fukuda, J. Hasegawa, M. Ishida, T. Nakajima, Y. Honda, O. Kitao, H. Nakai, M. Klene, J.X. Li, J.E. Knox, H.P. Hratchian, J.B. Cross, C. Adamo, J. Jaramillo, R. Gomperts, R.E. Stratmann, O. Yazyev, A.J. Austin, R. Cammi, C. Pomelli, J.W. Ochterski, P.Y. Ayala, K. Morokuma, G.A. Voth, P. Salvador, J.J. Dannenberg, V.G. Zakrzewski, S. Dapprich, A.D. Daniels, M.C. Strain, O. Farkas, D.K. Malick, A.D. Rabuck, K. Raghavachari, J.B. Foresman, J.V. Ortiz, Q. Cui, A.G. Baboul, S. Clifford, J. Cioslowski, B.B. Stefanov, G. Liu, A. Liashenko, P. Piskorz, I. Komaromi, R.L. Martin, D.J. Fox, T. Keith, M.A. Al-Laham, C.Y. Peng, A. Nanayakkara, M. Challacombe, P.M.W. Gill, B. Johnson, W. Chen, M.W. Wong, C. Gonzalez, J.A. Pople, Gaussian 03, Revision C.02, Gaussian Inc., Wallingford CT, 2004.
[48] J.B. Foresman, in: E. Frisch (Ed.), Exploring Chemistry with Electronic Structure Methods: A Guide to Using Gaussian, Gaussian, Pittsburg, PA, 1995.
[49] J.M.L. Martin, C. Van Alsenoy, GAR2PED Program, University of Antwerpen, Belgium, 1995.
[50] D.N. Sathyanarayana, D. Nicholls, Spectrochim. Acta 34A (1978) 263.
[51] J. Shukla, K.N. Upadhya, Indian J. Pure Appl. Phys. 11 (1973) 787.
[52] D. Hadzi, J. Jan, A. Ocvirk, Spectrochim. Acta 25A (1969) 97.
[53] G. Keresztury, M.P. Marzocchi, Spectrochim. Acta 31A (1975) 275.
[54] G. Keresztury, M.P. Marzocchi, Chem. Phys. 6 (1974) 117.
[55] L.K. Dyal, Spectrochim. Acta 44A (1988) 283.
[56] G. Varsanyi, Assignments for Vibrational Spectra of Seven Hundred Benzene Derivatives, New York, Wiley, 1974.
[57] K. Hanai, T. Okuda, T. Uno, K. Machida, Spectrochim. Acta 31A (1975) 1217.
[58] Y. Tanaka, Y. Tanaka, Y. Saito, K. Machida, Spectrochim. Acta 39A (1983) 159.
[59] T. Uno, K. Machida, K. Hanai, Spectrochim. Acta 22 (1966) 2065.
[60] N.P.G. Roeges, A Guide to the Complete Interpretation of Infrared Spectra of Organic Structures, New York, Wiley, 1994.
[61] N. Sundaraganesan, S. Ayyappan, H. Umamaheswari, B.D. Joshua, Spectrochim. Acta 66A (2007) 17.
[62] G. Socrates, Infrared Characteristic Group Frequencies, John wiley and Sons, New York, 1981.
[63] C. Lin, K. Wu, Chem. Phys. Lett. 321 (2000) 83.
[64] I. Yalcin, E. Sener, O. Ozden, A. Akin, Eur. J. Med.Chem. 25 (1990) 705.
[65] R. Saxena, L.D. Kandpaul, G.N. Mathur, J. Polym. Sci. A Polym. Chem. 40 (2002) 3959.
[66] R.M. Silverstein, G.C. Basseler, C. Morill, Spectrometric Identification of Organic Compounds, Wiley, New York, 2004.
[67] J.M. Engasser, C. Horvath, Biochem. J. 45 (1975) 43158.
[68] N.B. Colthup, L.H. Daly, S.E. Wiberly, Introduction to Infrared and Raman Spectroscopy, third ed., Academic Press, Boston, MA, 1990.
[69] S. Kundoo, A.N. Banerjee, P. Saha, K.K. Chattopadhyay, Mater. Lett. 57 (2003) 2193.
[70] L.G. Crane, D. Wang, L.M. Sears, B. Heynz, K. Carron, Anal. Chem. 67 (1995) 360.
[71] A.C.S. Bezerra, E.L. De Sa, F.C. Nart, J. Phys. Chem. 1013 (1997) 6443.
[72] M. El-Behery, H. El-Twigry, Spectrochim. Acta 66A (2007) 28.
[73] J. Coates, R.A. Meyers, Introduction to Infrared Spectrum, A Practical Approach, Chichester, John Wiley and Sons Ltd, 2000.
[74] P. Sett, N. Paul, S. Chattopadhyay, P.K. Mallick, J. Raman Spectrosc. 30 (1999) 277.
[75] P. Sett, S. Chattopadhyay, P.K. Mallick, Spectrochim. Acta 56A (2000) 855.
[76] P. Sett, S. Chattopadhyay, P.K. Mallick, J. Raman Spectrosc. 31 (2000) 177.
[77] J.H.S. Green, Spectrochim. Acta 24 (1968) 1627.
[78] S. Higuchi, H. Tsuyama, S. Tanaka, H. Kamada, Spectrochim. Acta 30A (1974) 463.
[79] K. Kohata, T. Fukuyama, K. Kuchitsu, J. Phys. Chem. 86 (1982) 602.
[80] V.A. Naumov, O.A. Litvionv, J. Mol. Struct. 99 (1983) 303.
[81] I. Kostava, N. Peica, W. Kiefer, J. Raman Spectrosc. 38 (2007) 2.
[82] H. Arslan, U. Florke, N. Kulcu, G. Binzet, Spectrochim. Acta 68A (2007) 1347.
[83] M.M. Candan, E. Kendi, M. Yarim, S. Sarac, M. Ertan, Anal. Sci. 17 (2001) 1023.
[84] Z. Gai, L.T. Qing, S.H. Lan, S.W. Hai, Z.J. She, G. Zhi-An, Chin. Struct. Chem. 4 (2005) 783.
[85] V. Krishnakumar, S. Muthunatesan, Spectrochim. Acta 66A (2007) 1082.
[86] B.N.B. Raj, M.R.P. Kurup, E. Suresh, Spectrochim. Acta 71A (2008) 1253.
[87] Y.R. Shen, The Principles of Nonlinear Optics, Wiley, New York, 1984.
[88] P.V. Kolinzky, Opt. Eng. 31 (1992) 1676.
[89] D.F. Eaton, Science 253 (1991) 281.
[90] C.R. Moylan, R.J. Twieg, V.Y. Lee, S.A. Swanson, K.M. Betterton, R.D. Miller, J. Am. Chem. Soc. 115 (1993) 12599.
[91] S. Gilmour, R.A. Montgomery, S.R. Marder, L.T. Cheng, A.K.Y. Jen, Y. Cai, J.W. Perry, L.R. Dalton, Chem. Mater. 6 (1994) 1603.
[92] M. Tommasini, C. Castiglioni, M. Del Zoppo, G. Zerbi, J. Mol. Struct. 480 (1999) 179.
[93] D.A. Kleinman, Phys. Rev. 126 (1962) 1977.
[94] S.M. Bakalova, A.G. Santos, I. Timcheva, J. Kaneti, I.L. Filipova, G.M. Dabrikov, V.D. Dimitrov, J. Mol. Struct. (Theochem.) 710 (2004) 229.
[95] Z.F. Dai, B.X. Peng, X.A. Chen, Dyes Pigments 40 (1999) 219.
[96] L. Ushakumari, C.Y. Panicker, H.T. Varghese, T. Ertan, I. Yildiz, J. Raman Spectrosc. 39 (2008) 1832.